

The design of a five-cell high-current superconducting cavity^{*}

LI Yong-Ming(李永明)¹ ZHU Feng(朱凤)^{1:1)} QUAN Sheng-Wen(全胜文)¹

Ali Nassiri² LIU Ke-Xin(刘克新)¹

¹ State Key Laboratory of Nuclear Physics and Technology,
Institute of Heavy Ion Physics, Peking University, Beijing 100871, China

² Advanced Photon Source, Argonne National Laboratory, 9700 S Cass Ave., Argonne, IL 60439, USA

Abstract: Energy recovery linacs are promising for achieving high average current with superior beam quality. The key component for accelerating such high-current beams is the superconducting radio-frequency cavity. The design of a 1.3 GHz five-cell high-current superconducting cavity has been carried out under cooperation between Peking University and the Argonne National Laboratory. The radio-frequency properties, damping of the higher order modes, multipacting and mechanical features of this cavity have been discussed and the final design is presented.

Key words: high current, superconducting cavity, higher order modes

PACS: 29.20.Ej **DOI:** 10.1088/1674-1137/36/1/013

1 Introduction

High average current electron beams based on energy recovery linacs (ERLs) have various applications. Multi-GeV electron beams are suitable for hard X-ray and electron-ion colliders, while energies below 100 MeV are adequate for long-wavelength ($\geq \mu\text{m}$) FEL and the electron cooling of ions. The superconducting radio frequency (SRF) cavity is one of the key components for accelerating high average current beams with superior beam quality. Major challenges for the high current superconducting cavity include emittance preservation of a high current beam, strong higher order mode (HOM) damping and high cryogenic loss at continuous-wave cavity operation.

The Argonne National Laboratory (ANL) and Peking University (PKU) are both interested in developing the high-current superconducting cavity. ANL is planning to update its Advanced Photon Source (APS) to hard X-ray in order to satisfy the future scientific requirements of the users. The planned ANL ERL-based light source promises much lower emittance and comparable beam currents to those used today [1]. For this purpose, ANL has designed a

1.4 GHz prototype five-cell high-current cavity [2]. In order to meet the availability of high-power RF sources, ANL asked PKU to make a prototype of the 1.3 GHz five-cell high-current superconducting cavity for pre-research of the APS update under the cooperation between ANL and PKU. In this paper, we describe the simulation and design of this cavity.

2 Cavity RF design

The TESLA-like cavity is known as the typical L-band superconducting cavity for accelerators with high acceleration gradient, such as the X-ray FEL and the International Linear Collider [3]. But the TESLA cavity is not suitable for high-current ERL because of the insufficient capability of HOM damping. Therefore, we decided to develop a high-current cavity for the pre-research of the APS update. In order to meet the requirement, the optimization of this high-current cavity focuses on effective damping of the HOMs, while maintaining appropriate R/Q of the accelerating π mode and an acceptable RF field level of B_p/E_{acc} or E_p/E_{acc} , where R is the shunt impedance and Q is the quality factor.

Received 12 April 2011

^{*} Supported by National High Technology Research and Development Program 863 (2009AA03Z206)

1) E-mail: zhufeng7726@pku.edu.cn

©2012 Chinese Physical Society and the Institute of High Energy Physics of the Chinese Academy of Sciences and the Institute of Modern Physics of the Chinese Academy of Sciences and IOP Publishing Ltd

The optimum design of an elliptical cavity is the consequence of compromises between RF and mechanical parameters. Usually, an elliptical cavity with good RF design faces mechanical problems such as Lorentz detune and pressure load. The geometric parameters for elliptical high current cavity (see Fig. 1) are the cell length (L), the radius at cell equator (R_{eq}), the radius at cell iris (R_{iris}), the equator ellipse ratio ($R_e = B/A$), the iris ellipse ratio ($r_i = b/a$), the distance from the cavity wall to the iris plane (d) and the side wall inclination (alpha).

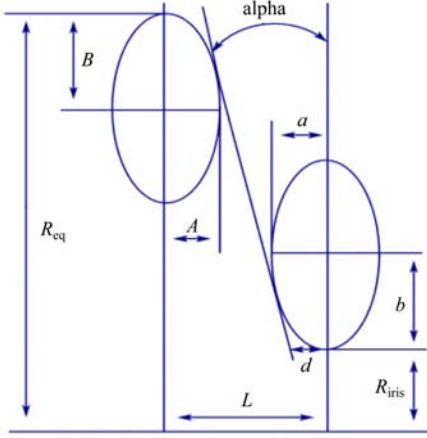


Fig. 1. The geometry parameters for a half cell.

For the mechanical design, good mechanical stiffness can reduce the effects of microphonics and Lorentz force detuning, while allowing a reasonable tuning capability. Alpha and d are dominating fac-

tors for mechanical stability. Not only do larger alpha and d increase cavity stiffness, but they also make the chemical treatment of internal surfaces easier.

For the RF design, L is determined by the fundamental resonant frequency f and beam velocity βc , $L = \beta c / (4f)$. R_{eq} is very sensitive to the resonant frequency, whereas it is insensitive to the other RF parameters and mechanical properties. R_{eq} is therefore used to tune the resonant frequency to the designed frequency. Fig. 2 shows the variation of the RF parameters as a function of R_{iris} , alpha, d and r_i simulated with the Superfish code [4]. As shown in Fig. 2(a), large R_{iris} could strengthen the cell coupling, whereas it increases E_p/E_{acc} and B_p/E_{acc} . It is found that it can significantly lower the impedances of HOMs, but it also reduces the impedances of the accelerating mode. Therefore, we should select the large R_{iris} ranging from 40 to 42 mm. Fig. 2(b) shows that alpha is not sensitive to R/Q , and small alpha will improve B_p/E_{acc} and cell coupling, but it increases E_p/E_{acc} . Considering the RF and mechanical properties, alpha should be from 14 to 18°. Fig. 2(c) shows that large d reduces E_p/E_{acc} , but it increases B_p/E_{acc} . So d is used to balance E_p/E_{acc} and B_p/E_{acc} for a cavity. In addition, small d has a good influence on the cell coupling. Considering the RF and mechanical properties, d should be selected from 0.6 to 0.8 mm. Fig. 2(d) shows that r_i is not sensitive to B_p/E_{acc} , R/Q and cell coupling. To minimize E_p/E_{acc} , the optimized r should be around 1.2–1.6.

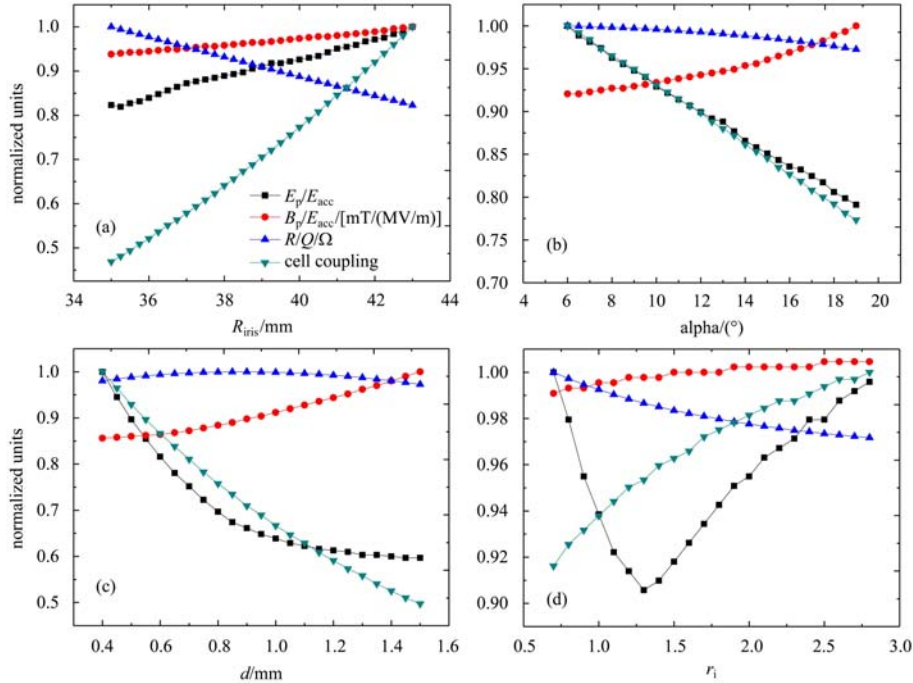


Fig. 2. RF parameters as a function of R_{iris} , alpha, d and r_i .

Based on the above analysis, the final optimized parameters of the five-cell high-current cavity are shown in Table 1. We adopt the asymmetric end cups design, which is beneficial for propagating the HOMs.

Table 1. The geometry parameters of the five-cell high current cavity.

parameters	mid-cell	left end cup	right end cup
L/mm	57.7	57.7	57.7
$R_{\text{iris}}/\text{mm}$	41.2	48.7	48.7
A/mm	38	35.7	40.4
B/mm	23.8	23.8	32.3
a/mm	10.8	16.9	15.6
b/mm	16.3	16.3	23
R_{eq}/mm	104	104	104
d/mm	6.9	13.1	11
$\alpha/(\text{°})$	17.2	14.8	13.6

The cutoff frequency of the beam pipe with a 48.7 mm radius is 1.81 GHz for the TE_{11} mode and 2.36 GHz for the TM_{01} mode. The frequencies of the first two passbands of the five-cell cavity HOMs are around 1.5 and 1.7 GHz, which are below the cutoff frequency of the beam pipe and can't be easily delivered externally. In order to propagate all the HOMs, we choose 60 mm as the enlarged beam pipe radius.

The five-cell high-current cavity and the field distribution along the axis calculated from the Superfish [4] program are shown in Fig. 3. Table 2 compares the fundamental mode RF parameters of the five-cell high-current cavity with the TESLA-type nine-cell cavity [5]. A large iris enhances the cell-to-cell coupling, which is good for propagating HOMs and

large frequency tolerance of each cell to obtain a flat- π mode, but it decreases R/Q per cell. Though the E_p/E_{acc} and B_p/E_{acc} are higher than those of the TESLA cavity, they are also acceptable, since the ERL high current cavity operates at the accelerating gradient of 15–20 MV/m [6].

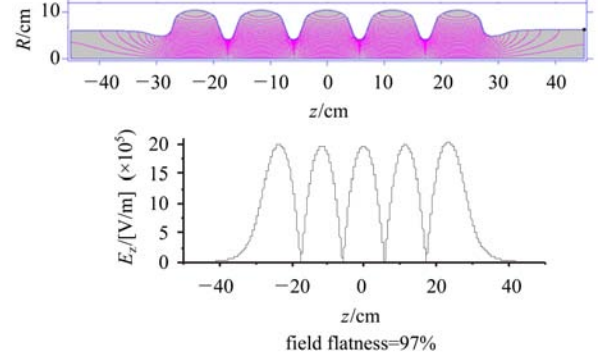


Fig. 3. Top: the electric field distribution of the fundamental π^- mode of the 1.3 GHz five-cell cavity calculated by Superfish; bottom: the on-axis field profile.

3 Higher order modes

The simulation of HOMs is finished with the Microwave Studio program [7]. The simulation model is shown in Fig. 4. A beam tube damper was used for coupling the HOMs. The Q_e was calculated assuming there are ideal RF absorbers at the end of the beam pipes and that all HOMs propagating through the waveguide ports will be absorbed completely.

Table 2. The RF parameter comparison of the different cavities.

cavity	f/MHz	I_b/mA	cell	$(R/Q)/\Omega$	E_p/E_{acc}	$(B_p/E_{\text{acc}})/[\text{mT}/(\text{MV}/\text{m})]$	coupling (%)	$R_{\text{iris}}/\text{mm}$	$R_{\text{pipe}}/\text{mm}$
TESLA	1300		9	1030	2	4.26	1.87	35	39
ANL- PKU	1300	100	5	462	2.4	4.6	3.8	41.2	60

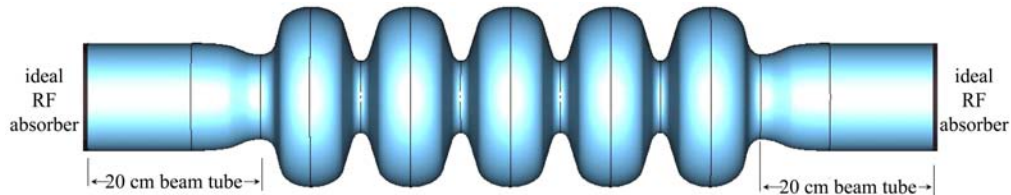


Fig. 4. The microwave studio model for Q_e calculation.

3.1 The monopole modes

The monopole HOMs will cause additional power loss on the superconducting cavity, bringing additional heat load to the liquid helium system and

increasing beam longitudinal emittance and energy spread. Monopole HOMs, whose frequency is close to bunch harmonic frequency, should be avoided as the beam power loss is extremely high in that situation [8]. For a total beam current I_b (100 mA) and

assuming an upper power limit of 200 W per mode, the impedance limit of the monopole mode close to $2N$ 1.3 GHz is [9]

$$\frac{R}{Q} \cdot Q_e < 10^4 \Omega, \quad (1)$$

where N is an integer. Fig. 5 gives the simulation result of monopole modes up to 5.5 GHz, where all monopole modes with frequencies close to beam harmonics are sufficiently damped with $(R/Q)Q_e < 10^4 \Omega$. The asymmetric end cells design is beneficial for propagating the HOMs, especially the dangerous trapped mode. The impedance of monopole HOMs in the symmetric design is higher than that in the asymmetric end cups design. In addition, there is a trapped mode near 3.9 GHz (3×1.3 GHz) and its $(R/Q)Q_e$ is about $10^5 \Omega$ in the symmetric design. However, with the asymmetric end cups design, the mode can easily propagate outside the cavity.

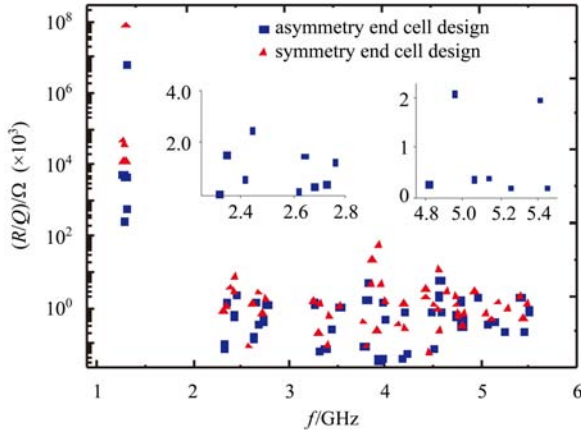


Fig. 5. The spectrum of the monopole modes.

Because there are no monopole modes close to the bunch harmonic frequency, the power dissipated in the cavity walls from the monopole HOMs excited by the beam is small. The power of all monopole HOMs in a cavity is proportional to the bunch charge Q_b , beam current I_b and the longitudinal loss factor $k_{//}$ [10]

$$P_{\text{HOM}} = k_{//} I_b Q_b - I_b Q_b \left[\frac{\omega R}{4Q_0} \right]_{\text{accl}}. \quad (2)$$

We used the ABCI code [11] to calculate the longitudinal loss factor of this cavity, and it is 7.62 V/pC for a 1 mm long Gaussian distribution bunch. For the APS update, if the bunch charge is 77 pC and average current is 100 mA, the total power of monopole HOMs will be 51.6 W per cavity. The power dissipated in the cavity walls for all monopole HOMs is calculated by

$$P_0 = P_{\text{HOM}} / (1 + Q_0 / Q_e). \quad (3)$$

The simulation shows that the Q_e of the monopole HOMs is less than 10^4 . Assuming that the Q_0 of all monopole HOMs is 10^9 , then the power dissipated in the cavity walls for all monopole HOMs is about 5 mW.

3.2 Dipole modes and quadrupole modes

Dipole modes and quadrupole modes have a deflecting field on the traverse axis. They are undesirable in accelerating cavities because they will increase the bunch emittance and energy spread, or even lead to beam breakup instability.

For a two-pass ERL concerning single dipole HOMs with arbitrary polarization angle α , the transverse beam breakup instability (BBU) threshold current is approximately given by the expression [12]

$$I_{\text{th}} = - \frac{2pc}{q \frac{\omega}{c} \left(\frac{R_d}{Q} \right) Q_e m_{12}^* \sin(\omega T_r)},$$

$$m_{12}^* = m_{12} \cos^2(\alpha) + (m_{14} + m_{32}) \sin \alpha \cos \alpha + m_{34} \sin^2 \alpha, \quad (4)$$

where p designates the beam momentum, $(R/Q)Q_e$ is the impedance of the higher order mode driving the instability, m_{12} , m_{14} and m_{32} are the transport matrix parameters and T_r is the bunch return time. From Eq. (4), a high current demands small R/Q and Q_e . Typical simulation results for the 100 mA high-current cavity calculated by Cornell University show that the dipole and quadrupole HOMs should meet the demands of Eq. (5) and Eq. (6) separately [9].

For the dipole HOMs,

$$\left(\frac{R}{Q} \right) \frac{Q_e}{f} < 1.4 \times 10^5 \frac{\Omega}{\text{cm}^2 \text{GHz}}. \quad (5)$$

For the quadrupole modes,

$$\left(\frac{R}{Q} \right) \frac{Q_e}{f} < 4 \times 10^6 \frac{\Omega}{\text{cm}^4 \text{GHz}}. \quad (6)$$

Our simulation results of the dipole modes and quadrupole modes are shown in Fig. 6. The $(R/Q)(Q_e/f)$ of the dipole modes and the quadrupole modes in our simulation is two orders less than the demands of the 100 mA limit in Eq. (5) and Eq. (6) separately. Therefore, a 100 mA BBU threshold current can be satisfied in a well designed ERL loop.

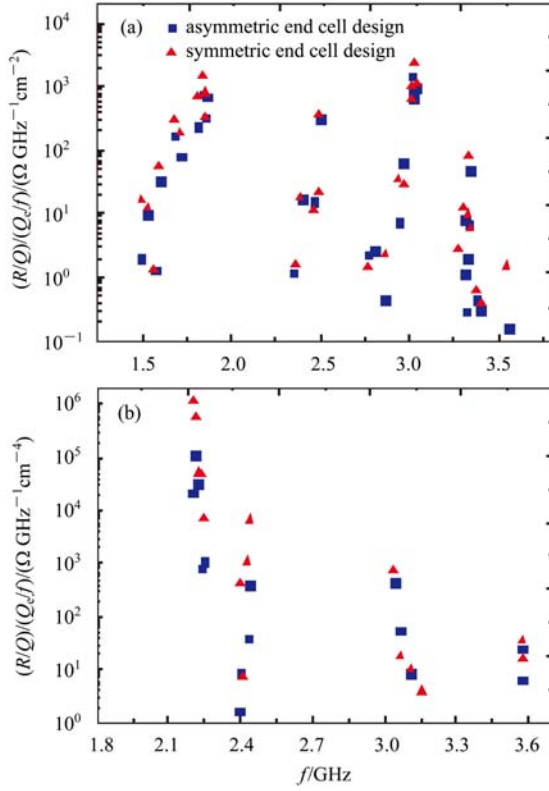


Fig. 6. The spectrum of the dipole HOMs (a); and the spectrum of the quadrupole HOMs (b).

4 Multipacting simulation

The multipacting effect occurs when electrons accelerated by the RF field are self-sustained via an electron avalanche caused by secondary electron emission. Multipacting currents can absorb RF energy and produce breakdown in high-power components such as couplers, windows and high-current SRF cavities [13]. To check the multipacting effect, we used the Multipac 2.1 code [14] to carry out the multipacting simulation of the cavity. Fig. 7 shows the enhanced counter function and the electron trajectory

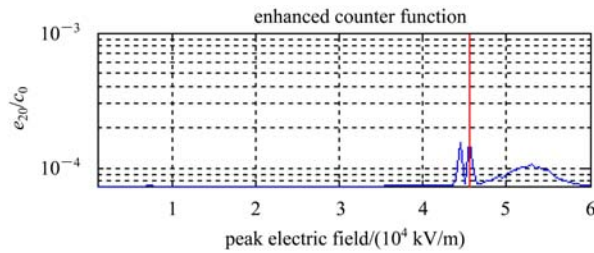


Fig. 7. The electron enhanced counter function, e_{20} , represents the number of secondary electrons after 20 impacts, and c_0 denotes the initial given number of electrons.

orbit of the optimized separately. The results indicate that the multipacting barrier can be processed for a good cavity surface.

5 The stiffening ring design

To decrease the influence of Lorentz force detuning and pressure load to the cavity, we optimized the stiffening rings of the 1.3 GHz five-cell cavity with the ANSYS and SUPERFISH codes. Fig. 8 provides a sketch of the stiffening ring acting on the mid-cup. Fig. 9 shows the change in mechanical properties with a change in the radius of the stiffening ring. From the simulation, the optimal radius of the stiffening rings is 58 mm for the mid-cell and 60 mm for both end-cups. With the designed stiffening ring, the Lorentz coefficient is $1.2 \text{ Hz}/(\text{MV}/\text{m})^2$. A 2 bar pressure load works on the cavity and the max stress is about $0.95 \text{ kgf}/\text{mm}^2$.

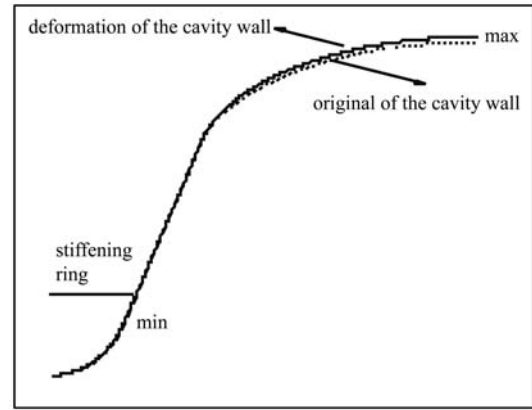


Fig. 8. The stiffening ring position on the mid-cup.

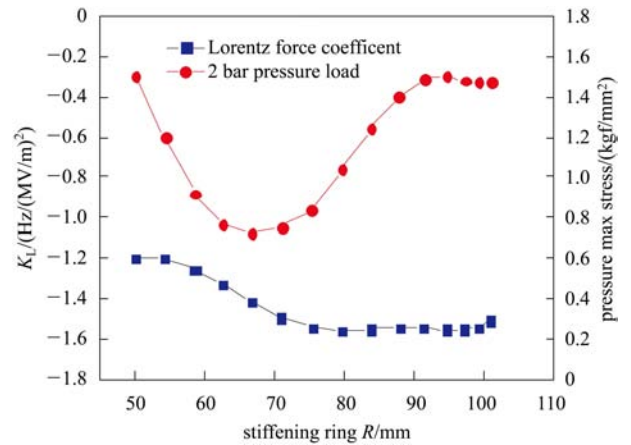


Fig. 9. The change in mechanical properties with a change in the radius of the stiffening ring.

6 Summary

The design of a 1.3 GHz high-current superconducting cavity for the pre-research of an APS, update has been completed under a collaboration between PKU and ANL. This prototype five-cell high-current cavity has a large iris and enlarged beam tube, which are beneficial for HOM propagation to the absorb-

ing material. Compared with the TESLA cavity, it has relatively high E_p/E_{acc} and B_p/E_{acc} , but is acceptable for ERL operation at an accelerating gradient of 15–20 MV/m. The RF property of this cavity meets the requirements for an APS update very well. The fabrication of the cavity has been finished and the cavity was sent to ANL waiting for cold RF test.

References

- 1 Borland M, Decker G et al. Configuration, Optics and Performance of a 7 GeV Energy Recovery Linac Upgrade for the Advanced Photo Source. In: PAC07. USA: New Mexico, 2007. <http://pac07.org/proceedings/PAPERS/TUPMN089.PDF>
- 2 LIU Zhen-Chao, Nassiri A, Waldschmidt G. Chinese Physics C(HEP & NP), 2010, **34**(5): 603
- 3 Hitoshi Hayano. Review of SRF Cavities for ILC, XFEL and ERL Applications. In: IPAC10. Japan: Kyoto, 2010. <http://accelconf.web.cern.ch/accelconf/IPAC10/papers/thxra02.pdf>
- 4 http://laacg1.lanl.gov/laacg/services/download_sf.phtml
- 5 Aune B et al. Phys. Rev. ST Accel., 2000 Beams 3: 092001
- 6 Umemori K, Furuya T et al. Design of L-Band Superconducting cavity for the Energy Recovery Linacs. In: APAC 2007. India: Indore, 2007. <http://accelconf.web.cern.ch/accelconf/a07/PAPERS/THC2MA03.PDF>
- 7 CST, <http://www.cst.com>.
- 8 Padamsee H, Knobloch J, Hays T. RF Superconductivity for Accelerators. New York: John Wiley & Sons, Inc., 1998. 337
- 9 Liepe M. Conceptual Layout of the Cavity String of the Cornell ERL Main Linac Cryomodule. In: SRF03, Germany: Lübeck, 2003, <http://accelconf.web.cern.ch/AccelConf/SRF2003/papers/mop33.pdf>
- 10 Liepe M, Knobloch J. Nucl. Instrum. Methods A, 2006, **557**: 354
- 11 ABCI, <http://abci.kek.jp/abci.htm>
- 12 Pozdeyev E. Phys. Rev. ST Accel. Beams, 2005, **8**: 054401
- 13 Padamsee H, Knobloch J, Hays T. RF Superconductivity for Accelerators. New York: John Wiley & Sons, Inc., 1998. 179–189
- 14 Ylä-Oijala P et al. MultiPac 2.1. Helsinki: Rolf Nevanlinna Institute, 2001